



Feature hiding in 3D human body scans[☆]

Joseph Laws¹
Nathaniel Bauernfeind¹
Yang Cai¹

¹*Ambient Intelligence Lab, CYLAB, Carnegie Mellon University, Pittsburgh, PA, U.S.A.*

Correspondence:

Yang Cai, Ambient Intelligence Lab,
CYLAB, Carnegie Mellon University,
4720 Forbes Avenue, Pittsburgh,
PA 15213, U.S.A.
Tel: +1412 268 5612;
Fax: +1412 268 7675;
E-mail: ycai@cmu.edu

Abstract

In this paper, we explore a privacy algorithm that detects human private parts in a 3D scan data set. The analogia graph is introduced to study the proportion of structures. The intrinsic human proportions are applied to reduce the search space in an order of magnitude. A feature shape template is constructed to match the model data points using Radial Basis Functions in a non-linear regression and the relative measurements of the height and area factors. The method is tested on 100 data sets from CAESAR database. Two surface rendering methods are studied for data privacy: blurring and transparency. It is found that test subjects normally prefer to have the most possible privacy in both rendering methods. However, the subjects adjusted their privacy measurement to a certain degree as they were informed of the context of security. *Information Visualization (2006) 5, 271–278.*

doi:10.1057/palgrave.ivs.9500136

Keywords: Human body; feature recognition; 3D scan; security; privacy

Introduction

The rapidly growing market of three-dimensional (3D) holographic imaging systems has created significant interest in possible security applications. Current devices operate using a millimeter wave transceiver to reflect the signal of the human body and any objects carried on it. The device penetrates less dense items, like clothing and hair. Unlike current metal detectors, the system can also detect non-metal threats or contraband, including plastics, liquids, drugs and ceramic weapons hidden under clothing as seen in Figure 1. The technology has also been used to create body measurements for custom-fit clothing. The holographic imager creates a high-resolution 3D body-scan, allowing shops to provide tailored measurements to designers or provide recommendations on best-fit clothing. These high-resolution scanned images reveal human body details and have raised privacy concerns. Airport and transport officials in several countries are refusing to run a test trial with the scanners until a more suitable way to conceal certain parts of the human body is found.¹

The scanner creates a 3D point cloud around the human body. As the millimeter wave signal cannot penetrate the skin, a 3D human surface can be found. Furthermore, since the typical pose of a subject is standing, with arms to the side, we can segment the 3-D data set into 2-D contours, which significantly reduces the amount of data processing. The goal of this study is to develop a method that can efficiently find and conceal the private parts of a human.

[☆]This paper was revised based on the published ICCS 2006 paper, "A Privacy Algorithm for 3D Human Body Scans", by Joseph Laws and Yang Cai, in LNCS 3994, Springer

Received: 20 January 2006
Revised: 21 July 2006
Accepted: 14 September 2006

Relevant studies

From the computer vision point of view, detecting features from 3D body scan data is nontrivial because human bodies are flexible and diversified.



Figure 1 The 3D holographic imaging systems can detect contraband beneath clothing, yet they raise privacy concerns due to the detailed human figure that is revealed.

Function fitting has been used for extracting special landmarks such as ankle joints from 3D body scan data,^{2,3} similar to the method for extracting special points on terrain.^{4,5} Curvature calculation is also introduced from other fields such as the sequence dependent DNA curvature.¹⁰ These curvature calculations use methods such as chain code,⁷ circle fit, ratio of end-to-end distance to contour length, ratio of moments of inertia, and cumulative and successive bending angles. Curvature values are calculated from the data by fitting a quadratic surface over a square window and calculating directional derivatives of this surface. Sensitivity to the data noise is a major problem in both function fitting and curvature calculation methods because typical 3D scan data contains noises. Template matching appears to be a promising method because it is invariant to the coordinate system.^{2,3} However, how to define a template and where to match the template is challenging and unique to each particular feature.^{6–27}

In summary, there are two major obstacles in this study: robustness and speed. Many machine learning algorithms are coordinate-dependent and limited by the training data space. Some algorithms only work within small bounding boxes that do not warrant an acceptable performance since the boxes need to be detected prior to the execution of the algorithm and are, often, not amenable to noise. For example, if a feature detection algorithm takes 1 hour to process, then it is not useful for a security screening system. In this paper, we present a fast and robust algorithm for privacy protection.

Analogia graph

Analogia (Greek: *αναλογία*, means ‘proportion’) graph is an abstraction of a proportion-preserving mapping of a

shape. Assume a connected non-rigid graph G , in which there is an edge with a length u . The rest of edges in G can be normalized as $p_i = v_i/u$. Let X and Y be metric spaces d_X and d_Y . A map $f: X \rightarrow Y$ is called Analogia Graph if for any $x, y \in X$ one has $d_Y(f(x), f(y))/u = d_X(x, y)/u$.

Analogia Graph is common in arts. The Russian Realism painter Ropin said that the secret of painting is ‘comparison, comparison and comparison.’ To represent objects in a picture realistically, a painter has to constantly measure and adjust the relationship among objects. ‘You should use the compass in your eyes, not in your hands,’ Ropin said. Instead of using absolute measurements of the distances and sizes, artists often use intrinsic landmarks inside the scene to estimate the relationships. For example, using a number of heads to estimate the height of a person and using a number of eyes to measure the length of a nose, and so on. Figure 2 is an Analogia Graph of a human body.

Using this artistic approach, we can create a graph where nodes represent regions and are connected to each other by edges, where the weight is defined as the distance between the nodes in proportion to the height of the head. Initially, we stretch the graph such that it overlays the entire body. We then create a link between each node and its respective counterpart. We link the head, shoulders, arms, elbows, hands, neck, breasts, waist, legs, knees, and feet to their respective regions. There is some tweaking required to assure that the waist region does indeed cover that area. Here, we run a quick top-down search through the plane slices until there are at least two disjoint areas, which we consider to be the middle of the waist. This change also makes modifications to where the knees and breasts are, and how large their regions are.

We take into account that not every subject has all four limbs. Our algorithm still accepts the scan if such items

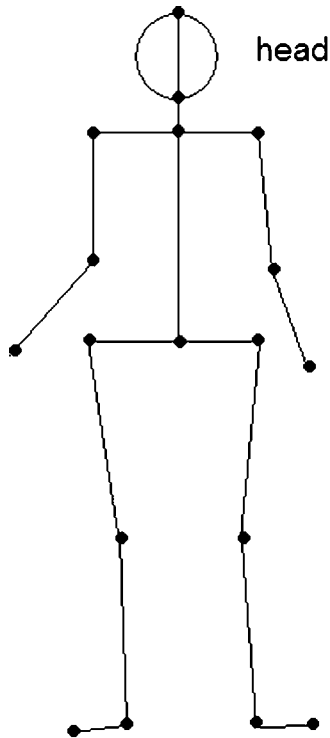


Figure 2 Analogia graph of a human figure.

are missing, such as half an arm or half a leg. It is also amenable to a complete loss of an arm or leg by looking at the expected ratio *vs* the real ratios when determining the length of each particular region.

However, convenient it is to find such broad range of regions, it is not possible to expand this algorithm to find more details like specific fingers, toes, ankle joints, or the nose. These searches are more complicated and require additional template fitting per feature and would significantly reduce the algorithm's run time.

We found that the intrinsic proportion method can reduce the search space in an order of magnitude. In addition, it reduces the risk of finding the local optima while searching the whole body.

Intrinsic proportions of humans

Our first step is to reduce the search space of the 3D body scans with the Analogia Graph. In this study, we assume that the body is standing with the arms hanging to the sides in a non-concealing way. If the arms are too close to the body, then the holograph imager cannot produce an accurate representation of the body and items on the side of the body could be completely missed because the area between the arm and the body would not be clearly defined. We start by dividing the 3D data points into 2D slices. The points are 'snapped' to the nearest planes enabling us to convert a 3D problem into a 2D one. Examining each slice from top to bottom is rather an expensive process. Here, we present a novel approach to reduce the search space by making use of intrinsic

proportions. It is a relative measurement that uses an object in the scene to measure other objects.⁸

Intrinsic proportion measurements have been used in architecture and art for thousands of years. Roman architect Vitruvius said that the proportions of a building should correspond to those of a person, and laid down what he considered to be the relative measurements of an ideal human. Similarly in art, the proportions of the human body in a statue or painting have a direct effect on the creation of the human figure. Artists use analogous measurements that are invariant to coordinate systems. For example, using the head to measure the height and width of a human body, and using an eye to measure the height and width of a face.

Figure 3 shows a sample of the vertical proportion in a typical art book and the actual distribution of head-to-body proportions calculated from our CAESAR data set.^{9,26} The results show that on average an adult human is six to eight heads tall. Based on our observations from one hundred 3D scan data sets of adults from 16 to 65 years old, including subjects from North America, Europe and Asia, we found that the length of one and a half head units from the bottom of the head is enough to cover the chest area. In addition, the chest width is about three heads wide. Figure 4 shows an output from the intrinsic proportion calculation based on the sample from CAESAR database.

Template matching

Template matching is an image registration process that matches a surface, of which all relevant information is known to a template of another surface. The matching of the two surfaces is driven by a similarity function. We need to solve two problems before applying template matching on the regions of interest. First, a suitable template has to be created. Second, a similarity function has to be selected so that a minimization algorithm can align the template onto the region of interest. For each plane of the scan data, the back of the body contour can be removed. By assigning the X-axis between the two points with the greatest distance, we can obtain the front part of the body contour. This aligns the subject to our template such that the matching is never attempted on a twisted or backward body. We then use three radial basis functions to configure the template for a female breast pattern.

$$y = \sum_{i=1}^3 a_i * \exp(-(x - s_i)^2), \quad (1)$$

where, $a = a_1 = a_2$, $b = a_3$, $s = s_1 = s_2$, and $s_3 = 0$. We use non-linear regression on the variables a , b , and s to match the template with the scan data. Figure 5 shows the matching results for the female and male samples.

Coordinate invariant measurements

Most shape descriptions depend on particular coordinate systems and particular viewpoints, meaning that the

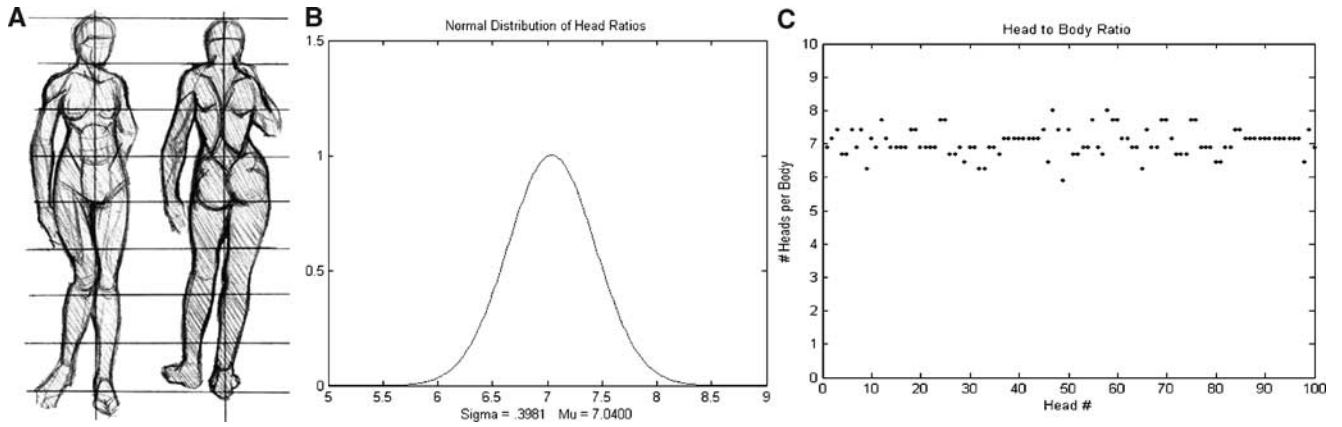


Figure 3 Body height measured by head example (A), normal distribution of heads per body (B), spread of actual number of heads per body size for 100 models (C).

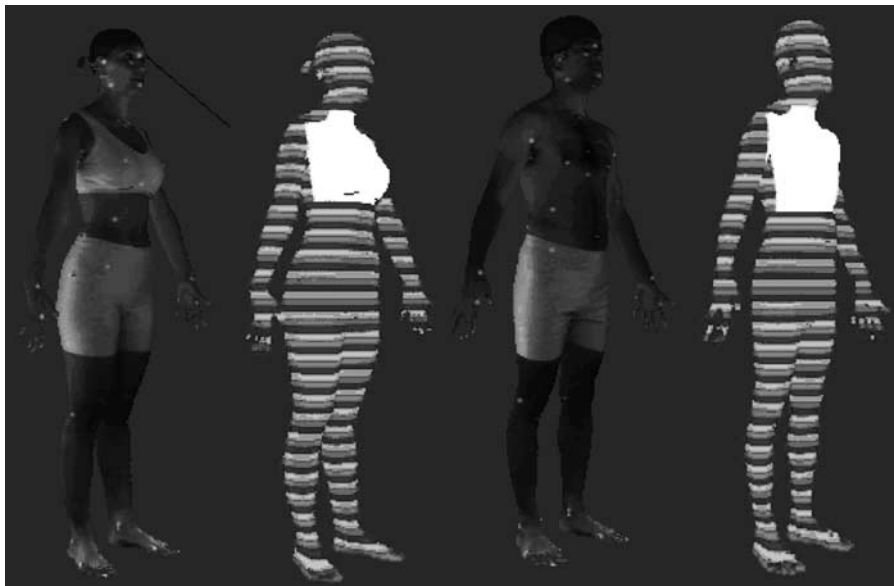


Figure 4 Using calculated ratios, the chest region is shown in white.

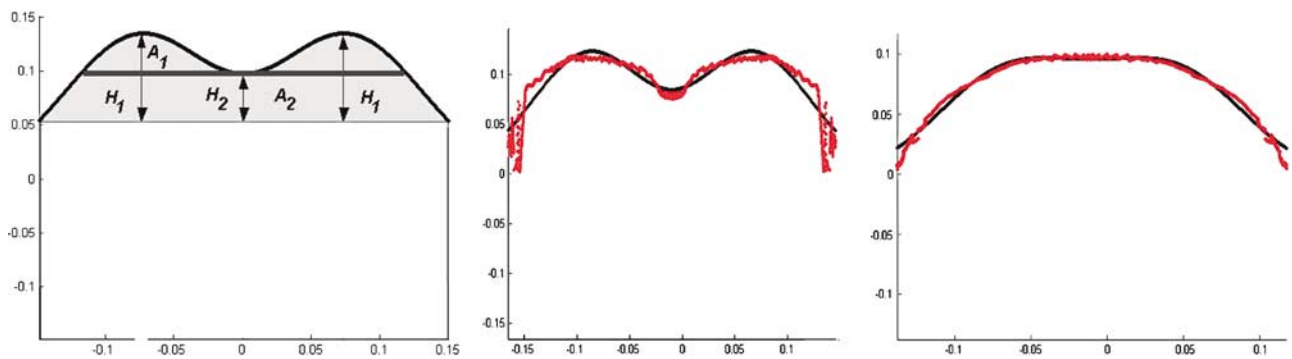


Figure 5 Variable definitions for the breast template (left), matching results for the female sample (middle) and male sample (right). The solid black curves are the template contours. The red points are the 3D scan data.

algorithm can only work within the same ‘space’ as the training data. Our shape invariant measurements are aimed to compute the shape properties from the ratio, rather than absolute values. This reduces this dependency onto a particular pose that is easily controlled, as opposed to creating an algorithm for each available holograph imager.

Template matching not only filters out noises, but also describes the characteristics of a shape. We define the following invariant similarity functions to the coordinate system: height ratio and area ratio. The height ratio is defined as:

$$H_r = \frac{H_1}{H_2} = \frac{Y_{mid/2}}{Y_{mid}}. \tag{2}$$

The area ratio is defined as the ratio of the area of curvature feature (A_1) to the total area (A_2) of the model by the following formula:

$$A_r = \frac{A_2}{A_1}, \tag{3}$$

where

$$A_2 = \int_l \sum_{i=1}^3 a_i * \exp(-(x - s_i)^2) dx, \tag{4}$$

$$A_1 = \int_l \left(\sum_{i=1}^3 a_i * \exp(-(x - s_i)^2) - c \right) dx, \tag{5}$$

$$c = \sum_{i=1}^3 a_i * \exp(-(mid - s_i)^2). \tag{6}$$

We use the Taylor series to find an appropriate approximation of the areas.

$$A_1 = \sum_{i=1}^3 a_i * \left(1 - (x - s_i)^2 + \frac{(x - s_i)^4}{2!} + \frac{(x - s_i)^6}{3!} + \frac{(x - s_i)^8}{4!} \right), \tag{7}$$

$$A_2 = \sum_{i=1}^3 a_i * \left(1 - (x - s_i)^2 + \frac{(x - s_i)^4}{2!} + \frac{(x - s_i)^6}{3!} + \frac{(x - s_i)^8}{4!} \right) - c. \tag{8}$$

It is necessary to attempt to match the template to each slice within the detected area, where only the greatest ratio of curvature is kept and used as the final result.

Results

We tested our algorithm with a subset of the CAESAR database, which contains 50 males and 50 females aged 16–65 years, where 50 of them are North American, 24 are

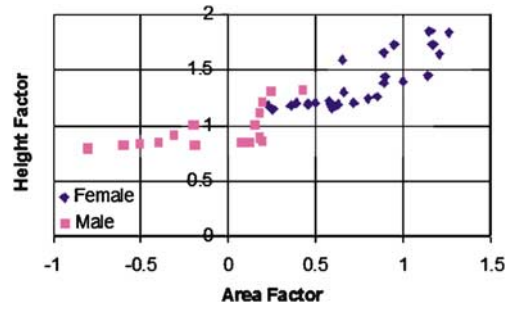


Figure 6 Classification test results with male and female samples.

Asian, and 26 are from the European survey of Italy and the Netherlands. We tested our algorithm to find the breast features from known female and male scan data samples. Figure 6 shows these test results. From the plot, we can see that there are two distinguishable groups, which happen to coincide with the particular gender of each subject. The male subjects tend to have no curvature features and lie in the lower left range of the graph, whereas female subjects do demonstrate these curvature features and lie in the upper right range of the graph. There is a ‘dilemma’ zone where some over-weight males do have the curvature features. However, the over-lapped zone is small, less than 8% of the total one hundred samples.

After the area and height factors have been calculated, we determine the feature area. Once we find the feature area, we reduce the polygon resolution so that the area is blurred. Figure 7 shows the results of the blurring effects in wire-frame mode. Figures 8 and 9 show scales of blurring and transparency, respectively.

Usability study

It is common knowledge that most people disagree on how much privacy can be given up for security. It was also another goal of ours to find out what most end-users would give up for that security. We ran two sets of two tests. Both sets included Figures 8 and 9 as scales where the subjects rated which they preferred, given the particular privacy concerns discussed prior to showing them the images. Ten random males and ten random females, ages from 19 to 59 were asked to participate in the study.

In the first study, subjects were told to imagine that they (or their girlfriend or wife) were in an airport and had to walk through the 3D holographic scanner, mentioned in the introduction, and that the resulted images would be displayed to the security officials on duty. They were asked to choose a blurred image, or a transparent image. The men averaged a 4.8 on the blurred scale and a 4.2 on the transparent scale. The women averaged a 4.0 on the blurred scale and a 3.8 on the transparent scale (Table 1).

In the second study, subjects were told to rate their privacy on a scale vs security in a context which not only

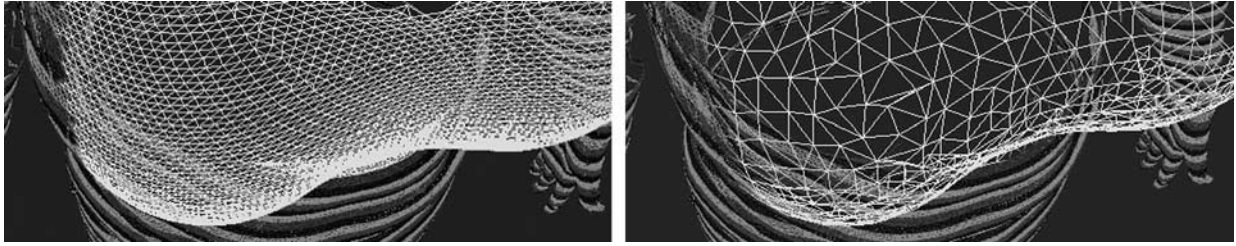


Figure 7 The blurred surface rendering.

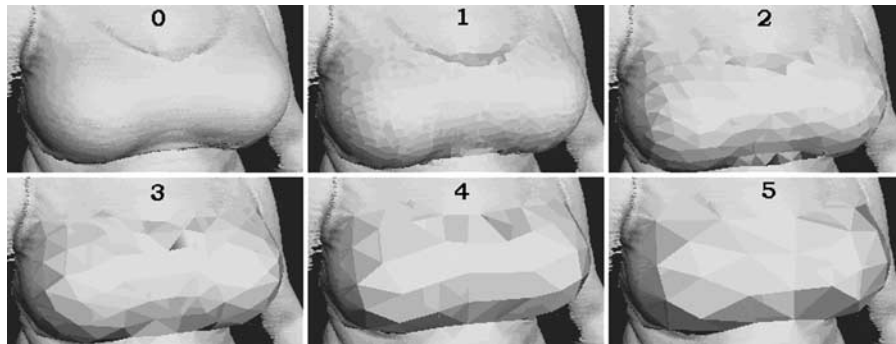


Figure 8 The blurred scale.

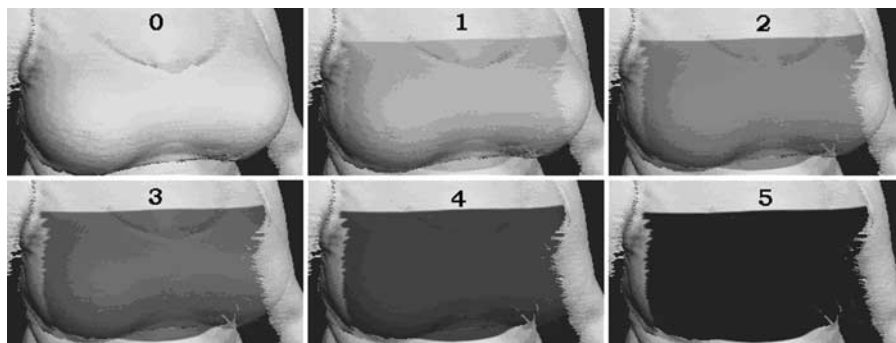


Figure 9 The transparent scale.

Table 1 User preferences without security concerns

| Gender | Method | Rank | | | | | | | | | | Average | |
|--------|--------------|------|---|---|---|---|---|---|---|---|---|---------|-----|
| Male | Blurring | 5 | 5 | 5 | 5 | 4 | 5 | 4 | 5 | 5 | 5 | 5 | 4.8 |
| | Transparency | 4 | 4 | 4 | 4 | 4 | 5 | 4 | 4 | 4 | 4 | 5 | 4.2 |
| Female | Blurring | 5 | 5 | 4 | 4 | 4 | 3 | 4 | 4 | 4 | 3 | 4.0 | |
| | Transparency | 5 | 5 | 4 | 4 | 4 | 4 | 3 | 3 | 4 | 2 | 3.8 | |

were they being observed, but others who may or may not be attempting to conceal weapons were also being observed. Such oddities as a pocketknife between the breasts would be more difficult to detect in a very blurred

mesh. The men averaged a 3.2 on the blurred scale and a 2.9 on the transparent scale. The women, on the other hand, averaged a 2.5 on the blurred scale and a 2.3 on the transparent scale (Table 2).

Table 2 User preferences with security concerns

| Gender | Method | Rank | | | | | | | | | | Average |
|--------|--------------|------|---|---|---|---|---|---|---|---|----|---------|
| | | 1 | 2 | 3 | 4 | 5 | 6 | 7 | 8 | 9 | 10 | |
| Male | Blurring | 4 | 3 | 3 | 3 | 5 | 3 | 2 | 3 | 3 | 3 | 3.2 |
| | Transparency | 3 | 3 | 3 | 3 | 4 | 3 | 2 | 3 | 3 | 2 | 2.9 |
| Female | Blurring | 2 | 3 | 3 | 2 | 2 | 2 | 2 | 3 | 3 | 3 | 2.5 |
| | Transparency | 2 | 2 | 3 | 2 | 2 | 2 | 2 | 3 | 3 | 2 | 2.3 |

The two studies display how different contexts can affect a subject's response and personal choice. It is clear that in the first study the men were more concerned about having their girlfriends/wives seen than the women concerned with how much they were seen. In the second study, it is clear that nearly every subject gave up more of their privacy to a certain degree for the benefits of security and the safety of their travels.

Conclusions

In this paper, we explored an algorithm to recognize body feature areas and hide them to protect a subject's privacy. The intrinsic human proportions are used to drastically reduce the search space and reduce the chance of local optima in detection. The Radial Basis Function is used as the feature template whose parameters are determined by non-linear regressions along each contour slice. Feature factors of the height and area are then used to classify the curvature feature as being male or female. The relative measurements are coordinate invariant, meaning that the algorithm is robust and is capable to work with multiple data sets. With the non-linear regression method, the template matching is effective and convergent within a given error range. We have tested one hundred body scans from the CAESAR database and found that the algorithm can successfully classify the male and female bodies based on the curvature features at a rate of over 90%.

Two surface rendering methods are studied for data privacy: blurring and transparency. It is found that test subjects normally prefer to have the most possible privacy in both rendering methods. However, the subjects adjusted their privacy measurement to a certain degree as they were informed of the context of security.

Our future work includes the development of more robust coordinate invariant methods to detect more predefined body features, and to calibrate the algorithms for both protecting privacy and detecting concealed weapons. Ultimately, we will work with the real field data to fine tune the algorithms.

Acknowledgments

The authors thank Cylab at Carnegie Mellon University for the support on security research and we are in debt to ARO for the research grant. We also appreciate the help from Alva Karl of Air Force for the CAESAR database.

References

- 1 Miller L, Feds wants see-through security. The Associated Press, June 25, 2003.
- 2 Suikerbuik CAM. Automatic feature detection in 3D human body scans. Master thesis INF/SCR-02-23, Institute of Information and Computer Sciences. Utrecht University, 2002.
- 3 Suikerbuik R, Tangelder H, Daanen H, Oudenhuijzen A. Automatic feature detection in 3D human body scans. *Proceedings of SAE Digital Human Modeling Conference*, 2004, 04-DHM-52.
- 4 Goldgof DB, Huang TS, Lee H. Curvature based approach to terrain recognition, Coordinating Science Laboratory University of Illinois, Urbana-Champaign, Tech. Note ISP-910, April 1989.
- 5 Goldgof DB, Huang TS, Lee H. Feature extraction and terrain matching. In: *Proceedings of the IEEE Computer Society Conference on Computer Vision Pattern Recognition*, Ann Arbor, MI, May 1988.
- 6 Fleck MM, Forsyth DA, Bregler C. Finding naked people. In: Buxton B, Cipolla R (Eds.), *Proceedings of the European Conference on Computer Vision*, Springer-Verlag: Berlin, Germany, 1996; 593–602.
- 7 Forsyth DA, Fleck MM. Automatic detection of human nudes. *International Journal of Computer Vision* 1999; **32**(1): 63–77.
- 8 Ratner P. *3-D Human Modeling and Animation*. John Wiley & Sons, Inc.: New York, 2003.
- 9 Anthropometry Resource (CAESAR), Final Report, Volume I: Summary, AFRL-HE-WP-TR-2002-0169, United States Air Force Research Laboratory, Human Effectiveness Directorate, Crew System Interface Division, 2255 H Street, Wright-Patterson AFB OH 45433-7022 and SAE International, 400 Commonwealth Dr., Warrendale, PA 15096.
- 10 Bansal M. Analysis of curvature in genomic DNA. <http://www.ibab.ac.in/bansal.htm>.
- 11 Besl PJ, Jain RC. Three-dimensional object recognition. *ACM Computer Surveys* 1985; **17**(1): 75–145.
- 12 Brady M, Ponce J, Yuille A, Asada H. Describing surfaces. *Computer Vision, Graphics, Image Processing* 1985; **32**: 1–28.
- 13 Calladine CR. *Gaussian Curvature and Shell Structures. The Mathematics of Surfaces*. Oxford University Press: Oxford, 1985. pp. 179–196.
- 14 Chen HH, Huang TS. Maximal matching of two three-dimensional point sets. In: *Proceedings of ICPR*, October 1986.
- 15 Coleman R, Burr M, Souvaine D, Cheng A. An intuitive approach to measuring protein surface curvature. *Proteins: structure function and bioinformatics* 1986; **61**: 1068–1074.
- 16 Fan TG, Medioni G, Nevatia R. Description of surfaces from range data using curvature properties. In: *Proceedings of CVPR*, May 1986.
- 17 Forsyth DA, Fleck MM. Body Plans, *Proceedings of the CVPR-97* 1997; 678–683.
- 18 Forsyth DA, Fleck MM. Identifying nude pictures, *Proceeding Third IEEE Workshop on Applications of Computer Vision* 1996; 103–108.
- 19 Gordon G. Face recognition based on depth and curvature features. *Proceedings of the IEEE Computer Society Conference on Computer Vision and Pattern Recognition* (Champaign, Illinois), 1992; 108–110.
- 20 Haralick RM, Sternberg SR, Zhuang X. Image analysis using mathematical morphology. *IEEE Transactions Pattern Analytical Machine Intelligence* 1987; **PAMI-9**: 532–550.
- 21 <http://www.dace.co.uk/proportion.htm>.



- 22 Jones PRM, Rioux M. Three-dimensional surface anthropometry: applications to the human body. *Optics and Lasers in Engineering* 1997; **28**: 89–117.
- 23 Li P, Corner BD, Paquette S. Evaluation of a surface curvature based landmark extraction method for three dimensional head scans. International Ergonomics Conference, Seoul, 2003.
- 24 Liu X, Kim W, Drerup B. 3D characterization and localization of anatomical landmarks of the foot, Proceeding (417), Biomedical Engineering, Acta Press, 2004, <http://www.actapress.com/PaperInfo.aspx?PaperID = 16382>.
- 25 Robinette KM, Blackwell S, Daanen HAM, Fleming S, Boehmer M, Brill T, Hoeflerlin D, Burnside D. Civilian American and European Surface Anthropometry Resource, 2002, http://www.hec.afrl.af_mil/HECP/card4a.shtml (online.2006).
- 26 Ioffe S, Forsyth DA. Probabilistic methods for finding people. *International Journal of Computer Vision* 2001; **43**: 45–68.
- 27 Sonka M, Boyle R, Hlavac V. Image processing, analysis and machine vision, PWS Publishing, Boston, USA, 1999.